Structural variants contribute to phenotypic variation in maize

Nathan S. Catlin[1,2,5*], Husain I. Agha[1,5], Adrian E. Platts[1], Manisha Munasinghe[3], Candice N. Hirsch[4], Emily B. Josephs[1,2,5*]

1 Department of Plant Biology, Michigan State University, East Lansing, MI, 48824, USA
2 Ecology, Evolution, and Behavior Program, Michigan State University, East Lansing, MI, 48824, USA
3 Department of Plant and Microbial Biology, University of Minnesota, St. Paul, MN, 55108, USA
4 Department of Agronomy and Plant Genetics, University of Minnesota, St. Paul, MN 55108, USA
5 Plant Resilience Institute, Michigan State University, East Lansing, MI, 48824, USA

*** catlinna@msu.edu, josep993@msu.edu**

Abstract

Comprehensively identifying the loci shaping trait variation has been challenging, in part because standard approaches often miss many types of genetic variants. Structural variants, especially transposable elements are likely to affect phenotypic variation but we need better methods in maize for detecting polymorphic structural variants and TEs using short-read sequencing data. Here, we used a whole genome alignment between two maize genotypes to identify polymorphic structural variants and then genotyped a large maize diversity panel for these variants using short-read sequencing data. We characterized variation of SVs within the panel and identified SV polymorphisms that are associated with life history traits and genotype-by-environment interactions. While most of the SVs associated with traits contained TEs, only one of the SV's boundaries clearly matched TE breakpoints indicative of a TE insertion, whereas the other polymorphisms were likely caused by deletions. All of the SVs associated with traits were in linkage disequilibrium with nearby single nucleotide polymorphisms (SNPs), suggesting that this method did not identify variants that would have been missed in a SNP association study.

Introduction

A central question of evolutionary biology is how different types of mutations – single nucleotide polymorphisms (SNPs), insertion-deletion polymorphisms, copy number variants, translocations, and transposable element insertions – shape the phenotypic diversity observed in nature. Much recent effort has focused on characterizing structural variants (SVs). Tens of thousands of SVs have been identified in plant genomes(Darracq *et al.*, 2018; Yang *et al.*, 2019; Schatz, 2018; Alonge *et al.*, 2020; Zhou *et al.*, 2022; Qin *et al.*, 2021). Specific SVs have been shown to affect important phenotypic traits in plants, including climate resilience in *Arabidopsis thaliana*, disease resistance and

domestication traits in maize and rice, and frost tolerance in wheat (Beló *et al.*, 2010; Cao *et al.*, 2011; Sieber *et al.*, 2016; Springer *et al.*, 2009; Xu *et al.*, 2012). In addition, maize SVs are predicted to be up to 18-fold enriched for alleles affecting phenotypes when compared to SNPs (Chia *et al.*, 2012).

A subset of SVs, transposable elements (TEs), are particularly interesting potential contributors to phenotypic variation (Lisch, 2013; Catlin and Josephs, 2022). TE content and polymorphism are shaped by a complex interplay of selection at the TE and organismal level (Charlesworth and Charlesworth, 1983; Ågren and Wright, 2011) and there are many examples of TE variation affecting phenotypes (Hirsch and Springer, 2017; Lisch, 2013). For example, a TE insertion in the regulatory region of the *teosinte branched1* (*tb1*) gene in maize enhances gene expression causing the upright branching architecture in maize compared to its progenitor, teosinte (Studer *et al.*, 2011). TE insertions also affect flesh color in grapes and fruit color and shape in tomato (Fray and Grierson, 1993; Kobayashi *et al.*, 2004; Van der Knaap *et al.*, 2004; Shimazaki *et al.*, 2011; Domínguez *et al.*, 2020). These phenotypic effects may result from changes in gene expression: TE activation can disrupt or promote gene expression (Hirsch and Springer, 2017; Fueyo *et al.*, 2022), and the industrial melanism phenotype in British peppered moths, *Biston betularia*, results from TE-induced overexpression of a gene responsible for pigment production (Hof *et al.*, 2016). TEs often activate (i.e. express and/or mobilize) in response to stress in many eukaryotes, including maize (Makarevitch *et al.*, 2015; Liang *et al.*, 2021), Arabidopsis (Wang *et al.*, 2022; Sun *et al.*, 2020), and *Drosophila melanogaster* (de Oliveira *et al.*, 2021; Milyaeva *et al.*, 2023), suggesting that they may contribute to trait variation in stressful environments. However, we lack systematic studies of how TEs in general affect phenotypic variation or how TEs may contribute to genotype-by-environment interactions outside of the context of stress.

Characterizing genomic variation for SVs and TEs has been challenging, especially in highly repetitive plant genomes where it is often difficult to uniquely align short-reads to the reference genome. Recent studies have shown that attempts to assemble SVs solely with short-read sequencing data can greatly underestimate the total number of SVs present in a population (Huddleston *et al.*, 2017; Audano *et al.*, 2019; Cameron *et al.*, 2019; Ebert *et al.*, 2021). Some estimates for the accuracy of SV discovery with short-read sequencing are as low as 11% in humans due to the inability of short-reads to align within highly repetitive regions, span large insertions, or concordantly align across SV boundaries (Lucas Lledó and Cáceres, 2013).

The increasing availability of long-read sequence has opened up an opportunity to identify SVs that would have been missed using short-read data. For example, long reads have been used to identify structural variants associated with traits in a set of 100 tomato accessions that were long-read sequenced (Alonge *et al.*, 2020). In other systems without enough long-read sequenced genotypes to directly look for associations between structural variants and phenotype, researchers have started with SVs detected in a smaller subset of individuals with reference assemblies and then genotyped a larger mapping panel of individuals with short-read sequencing data. Researchers have used pan-genome graph methods to identify SVs in a smaller number of reference sequences and then genotype in a larger sample of short-read sequenced genotypes in soybean (Liu *et al.*, 2020), rice (Qin *et al.*, 2021), and tomato (Zhou *et al.*, 2022). These studies have confirmed that SVs are important for trait heritability (Zhou *et al.*, 2022). However, graph genome approaches are challenging for plants with large genomes and have not yet been widely adopted. For example, a haplotype graph has been generated for 27 maize inbred lines, but not for a wider diversity panel (Franco *et al.*, 2020). Additionally, work using short-read alignments and pan-genome approaches have identified SVs in maize and found that SVs contributed to trait heritability and that approximately 60% were "related" to TEs but did not make clear links between SV

polymorphisms and TE insertions (Gui *et al.*, 2022) Plants with large genomes are not only important for a number of practical reasons, but they also may have different genetic architectures underlying trait variation that evolve differently (Mei *et al.*, 2018), so understanding how SVs and TEs contribute to trait variation in large-genomed plants is key for comprehensively understanding the importance of these variants in general.

To address the gap in understanding how structural variants contribute to trait variation in a species with a large genome, we used a simpler approach. We identified SVs found from the alignment of two reference assemblies, using short-reads that overlap the SV junctions. This approach has been used previously in tomato (Wang *et al.*, 2020). Here, we investigated the relationship between SV variation and phenotype in a diverse set of maize inbred lines in the Buckler-Goodman association panel. After identifying SVs that differ between two accessions, B73 and Oh43, we genotyped 277 maize lines present in a larger mapping panel for the SV alleles. We detected SV polymorphisms that varied across the panel and linked these polymorphisms to phenotypic variation and GxE.

Materials and Methods

1 Materials and methods

1.1 Structural variant identification

SVs between B73 and Oh43, called the "ascertainment set" from now on, were identified by Munasinghe *et al.* (2023). These genotypes were chosen to call SV presence/absence because they are both in the Buckler-Goodman association panel but come from different germplasm pools (Gage *et al.*, 2019). Ascertainment set SVs were filtered to only contain those that had 300 bps of colinear sequence determined by AnchorWave (Song *et al.*, 2022) in the immediate upstream and downstream regions flanking SV junctions. The sequence with the apparent insertion, including the 300 bp flanking genomic sequences, were extracted and combined to create a FASTA file containing "SV-present" alleles. The corresponding site in the genome where the SV was absent and 300 bp flanking genomic sequences were also extracted and combined in the final FASTA file to serve as the "SV-absent" allele sequence. Ultimately, this FASTA file was used as a set of pseudoreference alleles to call SV polymorphism in individuals with only short-read sequence data (Figure S1).

1.2 SV presence/absence genotyping

To call presence or absence for each SV, we collected genomic short-read data for 277 inbred maize genotypes from the Buckler-Goodman association panel sequenced for the third generation maize haplotype map (HapMap3) and aligned to the generated FASTA files with SV present and absent alleles (Flint-Garcia *et al.*, 2005; Bukowski *et al.*, 2018). Illumina adapters and low quality sequences were removed using Trimmomatic v0.39 (Bolger *et al.*, 2014). Surviving paired-end reads were merged into a master FASTQ file for each genotype and aligned to pseudoreference alleles using HISAT2 (Sirén *et al.*, 2014). PCR duplicate reads were also filtered out using the -r option within the *markdup* function in SAMtools v1.15.1 (Danecek *et al.*, 2021). The aligned data set was filtered to only contain concordant uniquely mapping reads. We used read-depth for each upstream and downstream SV boundary to support the presence or absence of SVs (Figure 1). Read coverage at each SV boundary was calculated using the coverage function within bedtools v2.30.0 (Quinlan and Hall, 2010).

First, we filtered out SVs where we were not able to use short-read data from B73 and Oh43 to correctly identify SV genotypes. For each SV, we required that: (1) upstream and downstream SV junctions have the same or higher read coverage from the genotype with the SV than the other genotype and (2) no reads spanning the insertion site for the genotype without the SV (Figure S2).

For the rest of the genotypes in the Buckler-Goodman association panel, SV-presence was supported in the query genotype if there was at least one read spanning the upstream or downstream SV junction and there was no read coverage at the SV polymorphic site for the alternative SV-absent allele. An SV-absent allele is supported if at least one read spans across the SV polymorphic site but no reads map to either SV junction of the corresponding SV-present allele. SVs are ambiguous if reads from the query genotype map to both the SV-present allele junctions and the SV-absent insertion site.

1.3 Calculating linkage disequilibrium between SNPs and SVs

SNPs for B73 in variant call format (VCF) were collected from the third generation maize haplotype map version 3.2.1 and coordinates were converted to the B73 NAM reference positions (version 5) using liftOverVCF in Picard tools (Pic, 2019; Qiu *et al.*, 2021). Chain files for the genome builds B73 version 3 (APGv3) to B73 version 4 (B73_RefGen_v4) and B73 version 4 to B73v5 (Zm-B73-REFERENCE-NAM-5.0) can be found in gramene.org and maizegdb.org, respectively (Tello-Ruiz *et al.*, 2022; Woodhouse *et al.*, 2021). We removed SNPs with more than 10% missing data, a minor allele frequency (MAF) of less that 10%, and those within SV regions, resulting in 13,551,774 SNPs in the final filtered dataset. Additionally, we appended polymorphic SV calls for each genotype in the HapMap3 dataset to the final VCF file. Because SV present alleles were characterized for both B73 and Oh43, we used the start of the SV coordinate for SV present alleles within B73 and the B73 insertion site for SVs present in Oh43 as the coordinate for LD analysis. Following methods from Qiu *et al.* (2021), we calculated LD between SNPs and nearby polymorphic SVs being sure to exclude SNPs inside of SVs, using PLINK v1.9 (Chang *et al.*, 2015),www.cog-genomics.org/plink/1.9/ with the following parameters: `--make-founders`, `--r2 gz dprime with-freqs`, `--ld-window-r2 0` , `--ld-window 1000000`, `--ld-window-kb 1000`, and `--allow-extra-chr`.

1.4 Association mapping

Polymorphic SVs across all query genotypes were converted to BIMBAM format (Servin and Stephens, 2007). SV-present alleles that were characterized as ambiguous were converted to absent calls. We performed a genome wide association (GWA) of SV PAVs using phenotypes from (Peiffer *et al.*, 2014) and (Bukowski *et al.*, 2018), with a linear mixed model (LMM) in GEMMA v0.98.03 (Zhou and Stephens, 2012). The traits tested were collected from Peiffer *et al.* (2014) and are best linear unbiased predictions of the following: growing degree days to silking, growing degree days to anthesis, growing degree days to anthesis-silking interval, days to silking, days to anthesis, anthesis-silking interval, plant height, ear height, difference of plant height and ear height, ratio of ear height and plant height, and ratio of plant height and days to anthesis. To account for missing genotypic data for each SV, we required at least 90% of the genotypes to have presence/absence calls for relatedness matrix calculations and subsequent associations. All Manhattan plots are shown with B73 coordinates, and Oh43 SV-present alleles were converted to B73 coordinates for display. To account for multiple-testing, we calculated a Bonferroni-adjusted significance threshold using the likelihood-ratio test(Bonferroni, 1936; Benjamini and Hochberg, 1995). P-values with $\alpha = 5\%$ were considered

significant. Filtered SNPs from the HapMap3 dataset were also subjected to GWA using the same methods as our polymorphic SV dataset.

In addition to the association analyses for main effects, we examined these data for genotype-by-environment interaction (GxE). For the 11 traits above, we used simple linear regression following the form of Finlay-Wilkinson (FW) regression (Finlay and Wilkinson, 1963) to record the slope (i.e. reaction norm) and mean squared error (MSE) for each genotype using the linear model (lm) function in R;

$$y_{ij} = \beta_0 + \beta_1 x_j + \epsilon_{ij},$$

where β_0 and β_1 are the intercept and slope estimates for the ith line, respectively, x_j is the average performance of all lines in the jth environment, and ϵ_{ij} is a random error term. We removed any lines which were not represented in at least 6 environments on a per trait basis to reduce the error in our estimates. This filtering resulted in a different number of individuals and markers used in each FW model (ranging from 245 to 274 individuals per trait). We then performed GWA of SV PAVs using slope and MSE estimates for each trait as quantitative phenotypes in GEMMA as before.

2 Results

2.1 Polymorphic SVs in the diversity panel

We genotyped SV polymorphisms for 277 maize genotypes at SVs segregating between B73 and Oh43 by aligning short reads from the genotypes to each SV allele and counting reads spanning genomic-SV junctions and SV polymorphic sites. Out of 98,422 polymorphic SVs between B73 and Oh43 (B73: 49,149, Oh43: 49,273), we were able to determine the genotype of 64,956 SVs in with short-read sequencing from the Buckler-Goodman association panel (Figure S2). Of these 64,956 SVs, the largest proportion were those classified as "TE = SV" (21,103, 32.5%), followed by "multi TE SVs" (18,326, 28.2%), "incomplete TE SVs" (10,928, 16.8%), "no TE SVs" (8,842, 13.6%), and "TE within SVs" (5,757, 8.9%) (Figures S3, S4). The proportions of SVs for each category are consistent with those prior to filtering ("TE = SV" (32,414, 32.9%), followed by "multi TE SVs" (26,689, 27.1%), "incomplete TE SVs" (19,013, 19.3%), "no TE SVs" (12,385, 12.6%), and "TE within SVs" (7,921, 8.0%), indicating little to no biases in our filtering method for each SV category. For more information about how SVs are classified into TE groupings, see Munasinghe *et al.* (2023).

For subsequent analyses, we filtered the SV dataset to only include variants with a minor allele frequency (MAF) $\geq$ 10% and presence/absence calls for more than 90% of genotypes, resulting in the retention 3,086 SV alleles (4.75% of dataset) (Figure S5). The frequency spectrum of the 3,086 SVs with MAF $\geq$ 10% was skewed towards moderate and high frequency insertions, as expected from conditioning on these SVs being polymorphic between two individuals (Figures 2, S3). For most SVs, the allele containing an insertion relative to the alternate allele was more common than alternate allele. This pattern is consistent with the polymorphism being caused by a deletion and the longer 'insertion' allele being the ancestral type. The frequency spectrum was relatively consistent across SV types (Munasinghe *et al.*, 2023).

Filtering on missing data and MAF removed many SVs because many individuals in the dataset have low realized sequencing coverage when mapped to the B73 reference assembly. There is a median coverage of 2.68, ranging from 0.031 in the A554 genotype to 19.47 in B57. Read depth per individual was negatively correlated with percent missing SV data per individual ($p = 2.4 \times 10^{-5}$) (Figures S6, S7), suggesting that missing data for SVs results from not having enough reads covering the junction sites.

This pattern suggests that this method needs a minimum of average read depth of 5 to successfully genotype SVs at most sites, although this number will likely vary by species.

SV genotypes are associated with phenotypic traits

In a genome-wide association analysis, SV presence/absence was associated with four out of the eleven traits tested: growing degree days to anthesis, days to silking, days to anthesis, and ear height (Figures 3,S8). All four SV associations detected contained TE sequences but none had boundaries that matched TE boundaries, suggesting that the polymorphisms were the result of deletions, not TE insertions.(Figure 4).

The SV associated with growing degree days to anthesis is within B73 on chromosome seven, 54 bp upstream of the B73 gene Zm00001eb330210 (syntenic with Oh43 gene Zm00039ab336990) (Figures 3, 4A). There are no currently known function for these genes in maize, nor their orthologs in other species including sorghum, foxtail millet, rice, or *Brachypodium distachyon*. There is evidence of increased expression in these genes in maize in whole seed, endosperm, and embryo for most 2-day increments post pollination (Walley *et al.*, 2016). This SV contained a mutator TE within it, but the SV boundaries did not match the TE boundaries.

The same SV polymorphism is associated with both days to silking and days to anthesis. This SV is present on chromosome three in Oh43 and is a large, ∼52kb multi-TE SV composed primarily of Ty3/Gypsy elements (Figures 3, 4B). This region is nearly 215 kb away from the nearest gene.

The SV associated with ear height contains a partial sequence of a mutator DNA transposon and is on Oh43 chromosome four within an intron of gene Zm00039ab208360 (syntenic with B73 gene Zm00001eb203840) (Figures 3, 4C). This gene, also called *traf42*, is a tumorreceptor-associated factor(TRAF) and codes for a BTB/POZ domain-containing protein *POB1*. Although TRAF domain containing proteins are ubiqutous across eukaryotes, there are far more genes encoding TRAF domains in plants compared to animals (Oelmüller *et al.*, 2005; Cosson *et al.*, 2010). In maize, *traf42* mediates protein-protein interactions (Dong *et al.*, 2017) and mutants of the maize gene ZmMAB1, which contains a TRAF domain and is exclusively expressed in the germline, causes chromosome segregation defects during meoisis (Juranić *et al.*, 2012). Additionally, *POB1* is involved in drought tolerance in the Antarctic moss, *Sanionia uncinata* (Park *et al.*, 2018).

SV genotypes are associated with GxE

We detected three significant associations between SV presence/absence and one of two measures of plasticity (FW regression slope and MSE) for three of the eleven traits tested: growing degree days to anthesis (MSE), ear height (slope), and the ratio of plant height and days to anthesis (MSE) (Figures 3, S9). All three SV sequences significantly associated with our plasticity metrics contained TE sequences and the SV on chromosome ten appeared to be directly caused by a TE insertion/deletion.

On chromosome four, we detected an association between an SV insertion in Oh43 and the MSE of the ratio of plant height to days to anthesis across growing locations. This SV contained a Ty3-like LTR retrotransposon but was not proximal to any gene models in either the Oh43 or B73 alignments.

On chromosome five, we detected an association between an SV insertion in B73 and the MSE of growing degree days to silking across growing locations. This SV contains a hAT TIR transposon but was not proximal to any gene model in either the Oh43 or B73 alignments.

On chromosome ten, we detected an association between an SV insertion in Oh43 and the slope of days to silking across growing locations which appeared to be caused by

a hAT TIR transposon. This TE was 713 bp from the uncharacterized Oh43 gene Zm00039ab424300 (a syntelog of B73 gene Zm00001eb415280).

Most SVs are in linkage disequilibrium with SNPs

All SV alleles used in the GWAS are within 1Mb from the nearest SNP present in the HapMap3 dataset (Figure S10) and all SVs have an $r^2 > 0.1$, with only 10 having an $r^2 < 0.5$. For the SV alleles that are significant to traits, all have a SNP in perfect LD.

Despite high LD between SVs and nearby SNPs, many of the associations detected between SVs and traits would not have been captured with a GWAS using all SNPs. Of the four SVs associated with main effects, none were found in the same peak regions in the SNP GWAS (Figures S11, S12). This lack of overlap between the SV GWAS associations and the SNP GWAS associations is a result of different significance cutoffs in the two different analyses. The HapMap3 SNP dataset has 16,435,136 SNPs while there were only 3,086 SVs in the SV association mapping analysis, so a SNP needed to have a p value below 3.04×10^{-9} to overcome the Bonferroni cut-off in the SNP GWAS while its linked SV needed a p value below 1.62×10^{-5} to be detected as significant in the SV GWAS.

Discussion

In this study we introduce a method leveraging short-read genomic data to capture SV diversity in a maize diversity panel. The maize genome's is highly repetitive nature, with upwards of 85% of transposable elements and other repeat sequences, makes relying on short-read alignments alone to characterize SV polymorphism *de novo* remains challenging (Hufford *et al.*, 2021). By ascertaining SVs presences/absences between two genotypes, we were able to call SVs across hundreds of maize genotypes using short-read data and identify SVs associated with trait variation.

We found seven SV polymorphisms associated with either average trait value or trait plasticity in a variety of maize phenotypes. These SV associations would not have been uncovered by using SNP datasets alone as shown using a SNP-only GWAS (Figure 3), supporting previous findings that SVs affecting phenotypic variation that would not be discovered in analyses that use SNPs alone (Yang *et al.*, 2019; Guo *et al.*, 2020; Hartmann, 2022; Zhang *et al.*, 2024). However, all SV associations detected here were in linkage disequilibrium with SNPs, so we did not detect associations that were not captured by the SNP dataset but instead these SVs were able to reach statistical significance because there were many fewer SVs than SNPs.

Of the SVs included in this study, 91% contained TEs or are themselves of TE origin and the largest category of SVs were clear examples of TE insertion (21,103 or 23.5%) . All of the SVs associated with trait variation and with GxE contained TE sequence, yet only the SV on chromosome ten for the slope of days to silking FW model appeared to be the direct result of TE insertions. The remaining six associations result from deletions that contain TEs. This result is consistent with previous findings that deletions have been the dominant contributors to SV polymorphism in maize (Munasinghe *et al.*, 2023).

We found three significant associations between SVs and mean squared error and slopes from the Finlay-Wilkinson regression models on three of the eleven traits tested. The finding that SVs associated with traits and with trait variation differed is consistent with previous work. For example, Finlay-Wilkinson regressions have been used previously in maize to show that the genetic architecture of trait means often differs across environments due to plasticity. (Kusmec *et al.*, 2017) Additional work in *Arabidopsis thaliana* has found that different loci are associated with reaction-norm

type measures of plasticity and variance measures of plasticity (Fournier-Level *et al.*, 2022). We did not see a clear pattern that SVs are more likely to affect trait variation than trait means.

Overall, we have demonstrated an approach for using two reference genomes to identify structural variants and then genotype for these variants in a larger panel of individuals with short-read sequencing data. This approach has allowed us to identify SVs associated with phenotypic variation and with GxE interactions. However, this approach does bias us towards common alleles that were polymorphic within the two reference assemblies. This bias is acceptable for a GWAS, where we will also be biased towards detecting associations with variants at intermediate allele frequency, but would be less appropriate for any analysis that would need to identify SVs with low allele frequencies. As long-read data becomes more affordable and there are more reference genomes available for more species, these types of approaches will improve our ability to detect SVs and investigate their potential functional importance.

Data availability

All sequencing data used is publicly available and generated by previous papers.

Acknowledgments

We thank Nathan Springer, Jeff Ross-Ibarra, Michelle Stitzer, and Yaniv Brandvain, along with members of the Josephs, Hirsch, and Ross-Ibarra lab for helpful comments and suggestions.

Funding

This work was supported by the National Science Foundation IOS-1934384 to E.B.J and a Postdoctoral Research Fellowship in Biology under Grant No. IOS-2010908 to M.M., National Institutes of Health R35-GM142829 to E.B.J, and USDA NIFA Project MICL02656 to E.B.J.

Conflicts of interest

The authors declare that they have no known competing financial interests or personal relationships that could have appeared to influence the work reported in this paper.

References

2019. Picard toolkit. `https://broadinstitute.github.io/picard/`.

Ågren JA, Wright SI. 2011. Co-evolution between transposable elements and their hosts: a major factor in genome size evolution. Chromosome research. 19:777–786.

Alonge M, Wang X, Benoit M, Soyk S, Pereira L, Zhang L, Suresh H, Ramakrishnan S, Maumus F, Ciren D *et al*. 2020. Major impacts of widespread structural variation on gene expression and crop improvement in tomato. Cell. 182:145–161.e23.

Audano PA, Sulovari A, Graves-Lindsay TA, Cantsilieris S, Sorensen M, Welch AE, Dougherty ML, Nelson BJ, Shah A, Dutcher SK *et al*. 2019. Characterizing the major structural variant alleles of the human genome. Cell. 176:663–675.

Beló A, Beatty MK, Hondred D, Fengler KA, Li B, Rafalski A. 2010. Allelic genome structural variations in maize detected by array comparative genome hybridization. Theor. Appl. Genet.. 120:355–367.

Benjamini Y, Hochberg Y. 1995. Controlling the false discovery rate: a practical and powerful approach to multiple testing. Journal of the Royal statistical society: series B (Methodological). 57:289–300.

Bolger AM, Lohse M, Usadel B. 2014. Trimmomatic: A flexible trimmer for illumina sequence data. Bioinformatics. 30:2114–2120.

Bonferroni C. 1936. Teoria statistica delle classi e calcolo delle probabilita. Pubblicazioni del R Istituto Superiore di Scienze Economiche e Commericiali di Firenze. 8:3–62.

Bukowski R, Guo X, Lu Y, Zou C, He B, Rong Z, Wang B, Xu D, Yang B, Xie C *et al*. 2018. Construction of the third-generation zea mays haplotype map. Gigascience. 7:1–12.

Cameron DL, Di Stefano L, Papenfuss AT. 2019. Comprehensive evaluation and characterisation of short read general-purpose structural variant calling software. Nature communications. 10:3240.

Cao J, Schneeberger K, Ossowski S, Günther T, Bender S, Fitz J, Koenig D, Lanz C, Stegle O, Lippert C *et al*. 2011. Whole-genome sequencing of multiple arabidopsis thaliana populations. Nat. Genet.. 43:956–963.

Catlin NS, Josephs EB. 2022. The important contribution of transposable elements to phenotypic variation and evolution. Current opinion in plant biology. 65:102140.

Chang CC, Chow CC, Tellier LC, Vattikuti S, Purcell SM, Lee JJ. 2015. Second-generation PLINK: rising to the challenge of larger and richer datasets. GigaScience. 4:s13742–015–0047–8.

Charlesworth B, Charlesworth D. 1983. The population dynamics of transposable elements. Genetics Research. 42:1–27.

Chia JM, Song C, Bradbury PJ, Costich D, De Leon N, Doebley J, Elshire RJ, Gaut B, Geller L, Glaubitz JC *et al*. 2012. Maize hapmap2 identifies extant variation from a genome in flux. Nature genetics. 44:803–807.

Cosson P, Sofer L, Hien Le Q, Léger V, Schurdi-Levraud V, Whitham SA, Yamamoto ML, Gopalan S, Le Gall O, Candresse T *et al*. 2010. Rtm3, which controls long-distance movement of potyviruses, is a member of a new plant gene family encoding a meprin and traf homology domain-containing protein. Plant physiology. 154:222–232.

Danecek P, Bonfield JK, Liddle J, Marshall J, Ohan V, Pollard MO, Whitwham A, Keane T, McCarthy SA, Davies RM *et al*. 2021. Twelve years of SAMtools and BCFtools. GigaScience. 10. giab008.

Darracq A, Vitte C, Nicolas S, Duarte J, Pichon JP, Mary-Huard T, Chevalier C, Bérard A, Le Paslier MC, Rogowsky P *et al*. 2018. Sequence analysis of european maize inbred line f2 provides new insights into molecular and chromosomal characteristics of presence/absence variants. BMC genomics. 19:1–20.

de Oliveira DS, Rosa MT, Vieira C, Loreto EL. 2021. Oxidative and radiation stress induces transposable element transcription in drosophila melanogaster. Journal of Evolutionary Biology. 34:628–638.

Domínguez M, Dugas E, Benchouaia M, Leduque B, Jiménez-Gómez JM, Colot V, Quadrana L. 2020. The impact of transposable elements on tomato diversity. Nat. Commun.. 11:4058.

Dong Z, Li W, Unger-Wallace E, Yang J, Vollbrecht E, Chuck G. 2017. Ideal crop plant architecture is mediated by tassels replace upper ears1, a btb/poz ankyrin repeat gene directly targeted by teosinte branched1. Proceedings of the National Academy of Sciences. 114:E8656–E8664.

Ebert P, Audano PA, Zhu Q, Rodriguez-Martin B, Porubsky D, Bonder MJ, Sulovari A, Ebler J, Zhou W, Serra Mari R *et al*. 2021. Haplotype-resolved diverse human genomes and integrated analysis of structural variation. Science. 372:eabf7117.

Finlay K, Wilkinson G. 1963. The analysis of adaptation in a plant-breeding programme. Australian journal of agricultural research. 14:742–754.

Flint-Garcia SA, Thuillet AC, Yu J, Pressoir G, Romero SM, Mitchell SE, Doebley J, Kresovich S, Goodman MM, Buckler ES. 2005. Maize association population: a high-resolution platform for quantitative trait locus dissection. Plant J.. 44:1054–1064.

Fournier-Level A, Taylor MA, Paril JF, Martínez-Berdeja A, Stitzer MC, Cooper MD, Roe JL, Wilczek AM, Schmitt J. 2022. Adaptive significance of flowering time variation across natural seasonal environments in arabidopsis thaliana. New Phytologist. 234:719–734.

Franco JAV, Gage JL, Bradbury PJ, Johnson LC, Miller ZR, Buckler ES, Romay MC. 2020. A maize practical haplotype graph leverages diverse nam assemblies. bioRxiv. pp. 2020–08.

Fray RG, Grierson D. 1993. Identification and genetic analysis of normal and mutant phytoene synthase genes of tomato by sequencing, complementation and co-suppression. Plant molecular biology. 22:589–602.

Fueyo R, Judd J, Feschotte C, Wysocka J. 2022. Roles of transposable elements in the regulation of mammalian transcription. Nature reviews Molecular cell biology. 23:481–497.

Gage JL, Vaillancourt B, Hamilton JP, Manrique-Carpintero NC, Gustafson TJ, Barry K, Lipzen A, Tracy WF, Mikel MA, Kaeppler SM *et al*. 2019. Multiple maize reference genomes impact the identification of variants by genome-wide association study in a diverse inbred panel. The plant genome. 12:180069.

Gui S, Wei W, Jiang C, Luo J, Chen L, Wu S, Li W, Wang Y, Li S, Yang N *et al*. 2022. A pan-zea genome map for enhancing maize improvement. Genome biology. 23:178.

Guo J, Cao K, Deng C, Li Y, Zhu G, Fang W, Chen C, Wang X, Wu J, Guan L *et al*. 2020. An integrated peach genome structural variation map uncovers genes associated with fruit traits. Genome biology. 21:1–19.

Hartmann FE. 2022. Using structural variants to understand the ecological and evolutionary dynamics of fungal plant pathogens. New Phytologist. 234:43–49.

Hirsch CD, Springer NM. 2017. Transposable element influences on gene expression in plants. Biochimica et Biophysica Acta (BBA)-Gene Regulatory Mechanisms. 1860:157–165.

Hof AEv, Campagne P, Rigden DJ, Yung CJ, Lingley J, Quail MA, Hall N, Darby AC, Saccheri IJ. 2016. The industrial melanism mutation in british peppered moths is a transposable element. Nature. 534:102–105.

Huddleston J, Chaisson MJ, Steinberg KM, Warren W, Hoekzema K, Gordon D, Graves-Lindsay TA, Munson KM, Kronenberg ZN, Vives L *et al*. 2017. Discovery and genotyping of structural variation from long-read haploid genome sequence data. Genome research. 27:677–685.

Hufford MB, Seetharam AS, Woodhouse MR, Chougule KM, Ou S, Liu J, Ricci WA, Guo T, Olson A, Qiu Y *et al*. 2021. De novo assembly, annotation, and comparative analysis of 26 diverse maize genomes.

Juranić M, Srilunchang Ko, Krohn NG, Leljak-Levanić D, Sprunck S, Dresselhaus T. 2012. Germline-specific math-btb substrate adaptor mab1 regulates spindle length and nuclei identity in maize. The plant cell. 24:4974–4991.

Kobayashi S, Goto-Yamamoto N, Hirochika H. 2004. Retrotransposon-induced mutations in grape skin color. Science. 304:982.

Kusmec A, Srinivasan S, Nettleton D, Schnable PS. 2017. Distinct genetic architectures for phenotype means and plasticities in zea mays. Nature plants. 3:715–723.

Liang Z, Anderson SN, Noshay JM, Crisp PA, Enders TA, Springer NM. 2021. Genetic and epigenetic variation in transposable element expression responses to abiotic stress in maize. Plant physiology. 186:420–433.

Lisch D. 2013. How important are transposons for plant evolution. Nature Reviews Genetics. 14:49–61.

Liu Y, Du H, Li P, Shen Y, Peng H, Liu S, Zhou GA, Zhang H, Liu Z, Shi M *et al*. 2020. Pan-genome of wild and cultivated soybeans. Cell. 182:162–176.

Lucas Lledó JI, Cáceres M. 2013. On the power and the systematic biases of the detection of chromosomal inversions by paired-end genome sequencing. PLoS One. 8:e61292.

Makarevitch I, Waters AJ, West PT, Stitzer M, Hirsch CN, Ross-Ibarra J, Springer NM. 2015. Transposable elements contribute to activation of maize genes in response to abiotic stress. PLoS genetics. 11:e1004915.

Mei W, Stetter MG, Gates DJ, Stitzer MC, Ross-Ibarra J. 2018. Adaptation in plant genomes. American journal of botany. 105:16–19.

Milyaeva PA, Kukushkina IV, Kim AI, Nefedova LN. 2023. Stress induced activation of ltr retrotransposons in the drosophila melanogaster genome. Life. 13:2272.

Munasinghe M, Read A, Stitzer MC, Song B, Menard C, Ma KY, Brandvain Y, Hirsch CN, Springer N. 2023. Combined analysis of transposable elements and structural variation in maize genomes reveals genome contraction outpaces expansion.

Oelmüller R, Peškan-Berghöfer T, Shahollari B, Trebicka A, Sherameti I, Varma A. 2005. Math domain proteins represent a novel protein family in arabidopsis thaliana, and at least one member is modified in roots during the course of a plant–microbe interaction. Physiologia Plantarum. 124:152–166.

Park M, Hong SG, Park H, Lee Bh, Lee H. 2018. Identification of reference genes for rt-qpcr in the antarctic moss sanionia uncinata under abiotic stress conditions. Plos one. 13:e0199356.

Peiffer JA, Romay MC, Gore MA, Flint-Garcia SA, Zhang Z, Millard MJ, Gardner CAC, McMullen MD, Holland JB, Bradbury PJ *et al*. 2014. The genetic architecture of maize height. Genetics. 196:1337–1356.

Qin P, Lu H, Du H, Wang H, Chen W, Chen Z, He Q, Ou S, Zhang H, Li X *et al*. 2021. Pan-genome analysis of 33 genetically diverse rice accessions reveals hidden genomic variations. Cell. 184:3542–3558.

Qiu Y, O'Connor CH, Della Coletta R, Renk JS, Monnahan PJ, Noshay JM, Liang Z, Gilbert A, Anderson SN, McGaugh SE *et al*. 2021. Whole-genome variation of transposable element insertions in a maize diversity panel. G3. 11.

Quinlan AR, Hall IM. 2010. Bedtools: a flexible suite of utilities for comparing genomic features. Bioinformatics. 26:841–842.

Schatz M. 2018. Michael schatz: 100 genomes in 100 days: The structural variant landscape in tomato genomes. Nanopore Community Meeting 2018.

Servin B, Stephens M. 2007. Imputation-based analysis of association studies: candidate regions and quantitative traits. PLoS genetics. 3:e114.

Shimazaki M, Fujita K, Kobayashi H, Suzuki S. 2011. Pink-colored grape berry is the result of short insertion in intron of color regulatory gene. PLoS One. 6:e21308.

Sieber AN, Longin CFH, Leiser WL, Würschum T. 2016. Copy number variation of cbf-a14 at the fr-a2 locus determines frost tolerance in winter durum wheat. Theoretical and Applied Genetics. 129:1087–1097.

Sirén J, Välimäki N, Mäkinen V. 2014. HISAT2-fast and sensitive alignment against general human population. IEEE/ACM Trans. Comput. Biol. Bioinform.. 11:375–388.

Song B, Marco-Sola S, Moreto M, Johnson L, Buckler ES, Stitzer MC. 2022. AnchorWave: Sensitive alignment of genomes with high sequence diversity, extensive structural polymorphism, and whole-genome duplication. Proc. Natl. Acad. Sci. U. S. A.. 119.

Springer NM, Ying K, Fu Y, Ji T, Yeh CT, Jia Y, Wu W, Richmond T, Kitzman J, Rosenbaum H *et al*. 2009. Maize inbreds exhibit high levels of copy number variation (cnv) and presence/absence variation (pav) in genome content. PLoS genetics. 5:e1000734.

Studer A, Zhao Q, Ross-Ibarra J, Doebley J. 2011. Identification of a functional transposon insertion in the maize domestication gene tb1. Nat. Genet.. 43:1160–1163.

Sun L, Jing Y, Liu X, Li Q, Xue Z, Cheng Z, Wang D, He H, Qian W. 2020. Heat stress-induced transposon activation correlates with 3d chromatin organization rearrangement in arabidopsis. Nature communications. 11:1886.

Tello-Ruiz MK, Jaiswal P, Ware D. 2022. Gramene: a resource for comparative analysis of plants genomes and pathways, In: , Springer. pp. 101–131.

Van der Knaap E, Sanyal A, Jackson S, Tanksley S. 2004. High-resolution fine mapping and fluorescence in situ hybridization analysis of sun, a locus controlling tomato fruit shape, reveals a region of the tomato genome prone to dna rearrangements. Genetics. 168:2127–2140.

Walley JW, Sartor RC, Shen Z, Schmitz RJ, Wu KJ, Urich MA, Nery JR, Smith LG, Schnable JC, Ecker JR *et al*. 2016. Integration of omic networks in a developmental atlas of maize. Science. 353:814–818.

Wang X, Gao L, Jiao C, Stravoravdis S, Hosmani PS, Saha S, Zhang J, Mainiero S, Strickler SR, Catala C *et al*. 2020. Genome of solanum pimpinellifolium provides insights into structural variants during tomato breeding. Nature communications. 11:5817.

Wang Y, Liu Y, Qu S, Liang W, Sun L, Ci D, Ren Z, Fan LM, Qian W. 2022. Nitrogen starvation induces genome-wide activation of transposable elements in arabidopsis. Journal of Integrative Plant Biology. 64:2374–2384.

Woodhouse MR, Cannon EK, Portwood JL, Harper LC, Gardiner JM, Schaeffer ML, Andorf CM. 2021. A pan-genomic approach to genome databases using maize as a model system. BMC plant biology. 21:1–10.

Xu X, Liu X, Ge S, Jensen JD, Hu F, Li X, Dong Y, Gutenkunst RN, Fang L, Huang L *et al*. 2012. Resequencing 50 accessions of cultivated and wild rice yields markers for identifying agronomically important genes. Nat. Biotechnol.. 30:105–111.

Yang N, Liu J, Gao Q, Gui S, Chen L, Yang L, Huang J, Deng T, Luo J, He L *et al*. 2019. Genome assembly of a tropical maize inbred line provides insights into structural variation and crop improvement. Nat. Genet.. 51:1052–1059.

Zhang Z, Viana JPG, Zhang B, Walden KK, Paul HM, Moose SP, Morris GP, Daum C, Barry KW, Shakoor N *et al*. 2024. Major impacts of widespread structural variation on sorghum. Genome Research. 34:286–299.

Zhou X, Stephens M. 2012. Genome-wide efficient mixed-model analysis for association studies. Nat. Genet.. 44:821–824.

Zhou Y, Zhang Z, Bao Z, Li H, Lyu Y, Zan Y, Wu Y, Cheng L, Fang Y, Wu K *et al*. 2022. Graph pangenome captures missing heritability and empowers tomato breeding. Nature. 606:527–534.

Figures

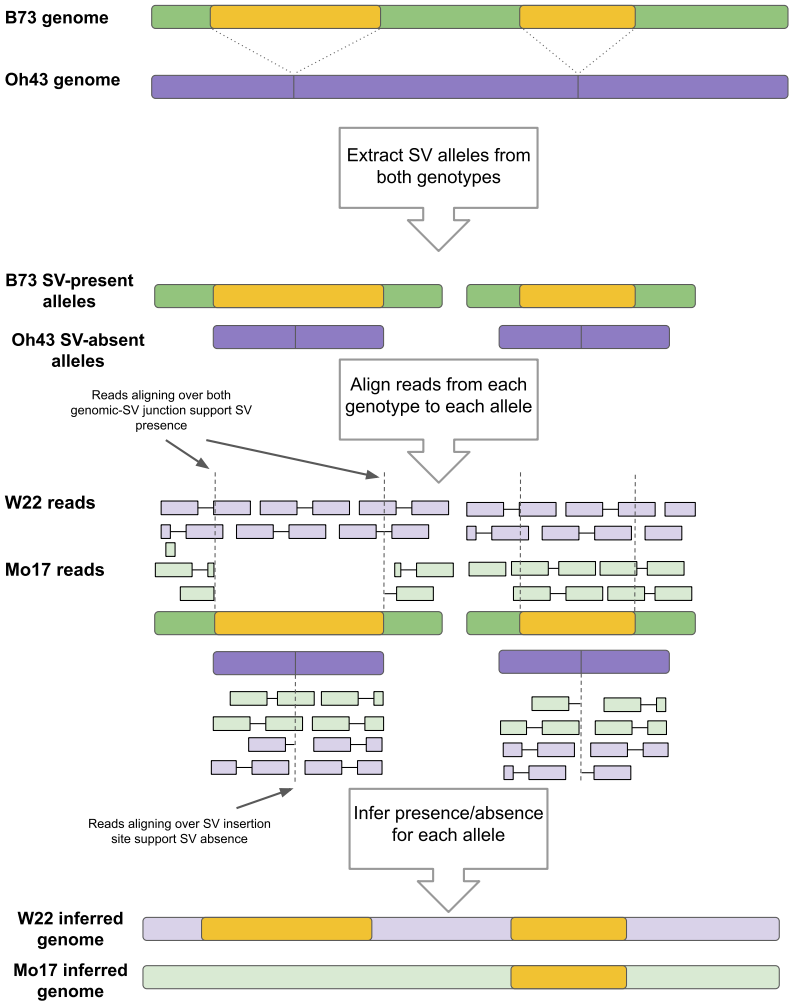

Figure 1. Method to call SV presence/absence with short read genomic data. Using B73 and Oh43 as our ascertainment set, we must first find polymorphic SVs between these two genotypes. To significantly improve read-mapping runtimes, we extract SVs and adjacent genomic sequences where SVs are present, while extracting only adjacent genomic regions at the polymorphic site where the SV is absent in the opposite genotype — termed pseudoreference SV alleles. Next, reads from a genotype of interest are mapped to these generated sequences. SVs can then be inferred present or absent based on their alignment to either allele.

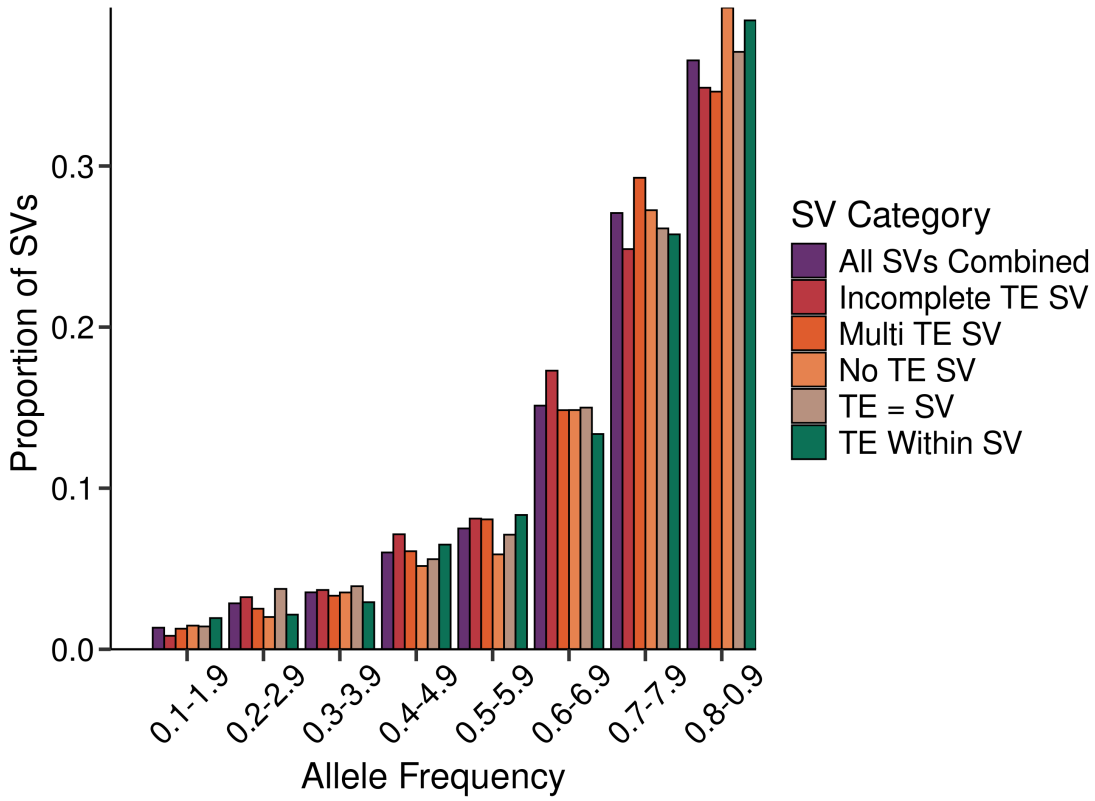

Figure 2. Site-frequency Spectrum of Unimputed SVs SVs were filtered to only contain those with a minor allele frequency $\geq$ 10% and less than 10% missing data (n = 3,086). The SFS is unfolded and displays the frequency of the allele with the putative insertion (or that is lacking a deletion).

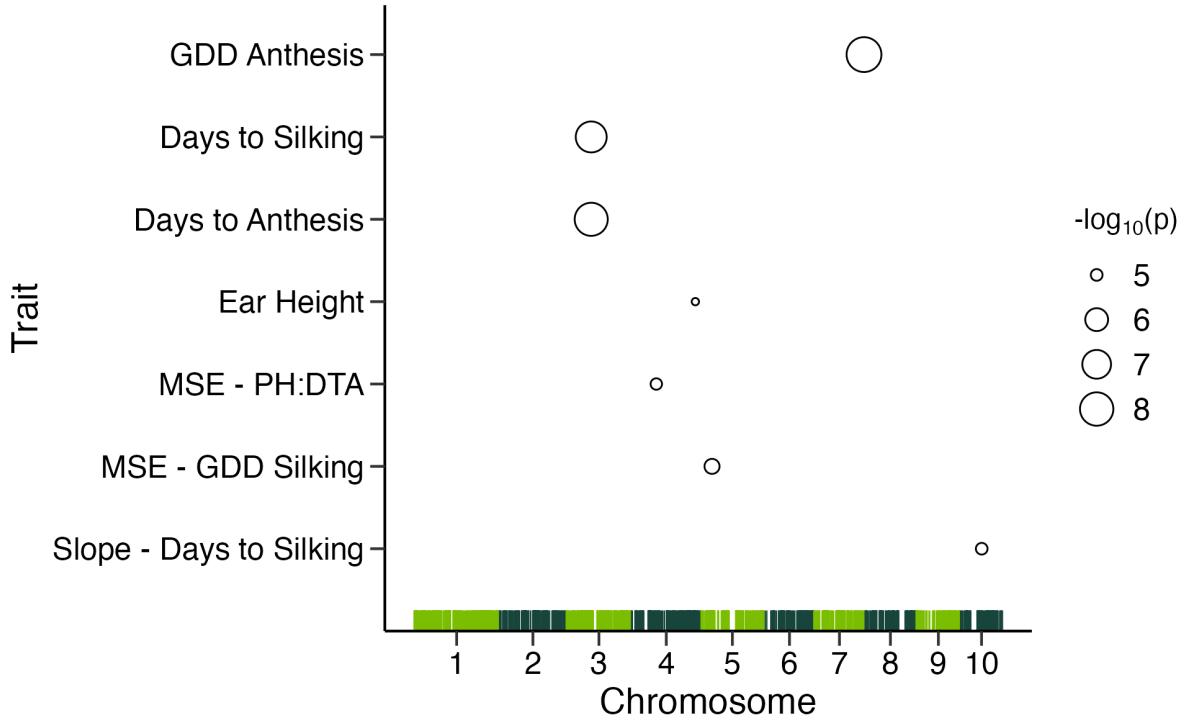

Figure 3. Genomic position and p values for seven traits with significant SV presence/absence associations. Bars along bottom represent the genomic positions for the 3,086 SV markers used in the association panel, with chromosomes in alternating colors. Points are sized according to the $-log_{10}(p)$. The Bonferroni-corrected alpha was equal to a $-log_{10}(p)$ of 4.8 (GDD: growing degree days; MSE: mean squared error; PH:DTA: ratio of plant height to days to anthesis).

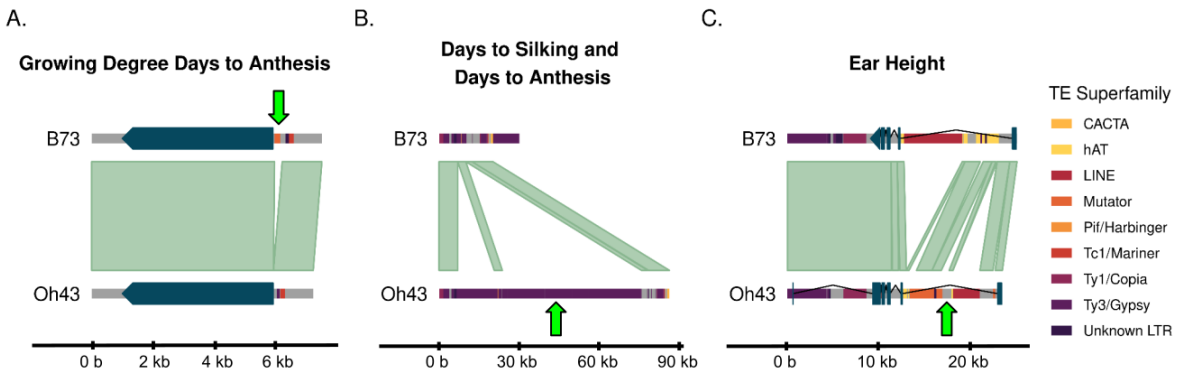

Figure 4. Trait associated structural variant polymorphisms between B73 and Oh43. Green arrows point to polymorphic SV regions. Alignable regions are shown as green bars between genotypes. **(A)**. A mutator TE within an SV is present in B73 and absent in Oh43 . This SV is 54 bp upstream of the B73 gene Zm00001eb330210, syntenic with Oh43 gene Zm00039ab336990.**(B)**. A large SV containing multiple Ty3/Gypsy TEs is present in Oh43 and absent in B73. This intergenic SV is approximately 215 kb from the nearest gene.**(C)**. A polymorphic incomplete TE - SV is located within the Oh43 gene Zm00039ab208360 is present in Oh43 and absent in B73.

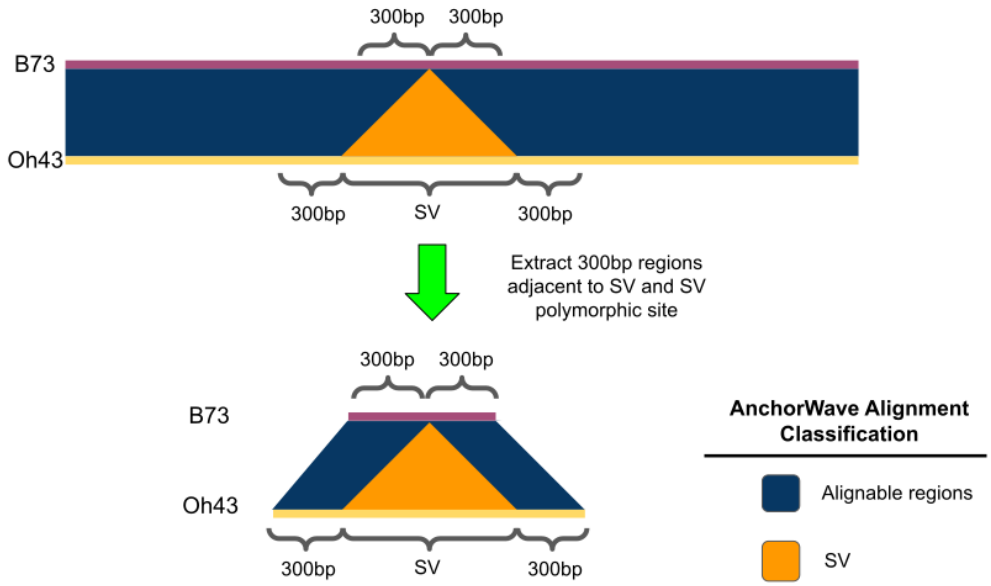

Figure S1. Extracting SV present and absent alleles – For each polymorphic SV between B73 and Oh43 identified in Munasinghe *et al.* (2023), we extracted 300 bp flanking alignable regions along with the SV for to make "SV present alleles" while 300 bp flanking alignable regions were extracted around the insertion point, which we term "SV-absent alleles".

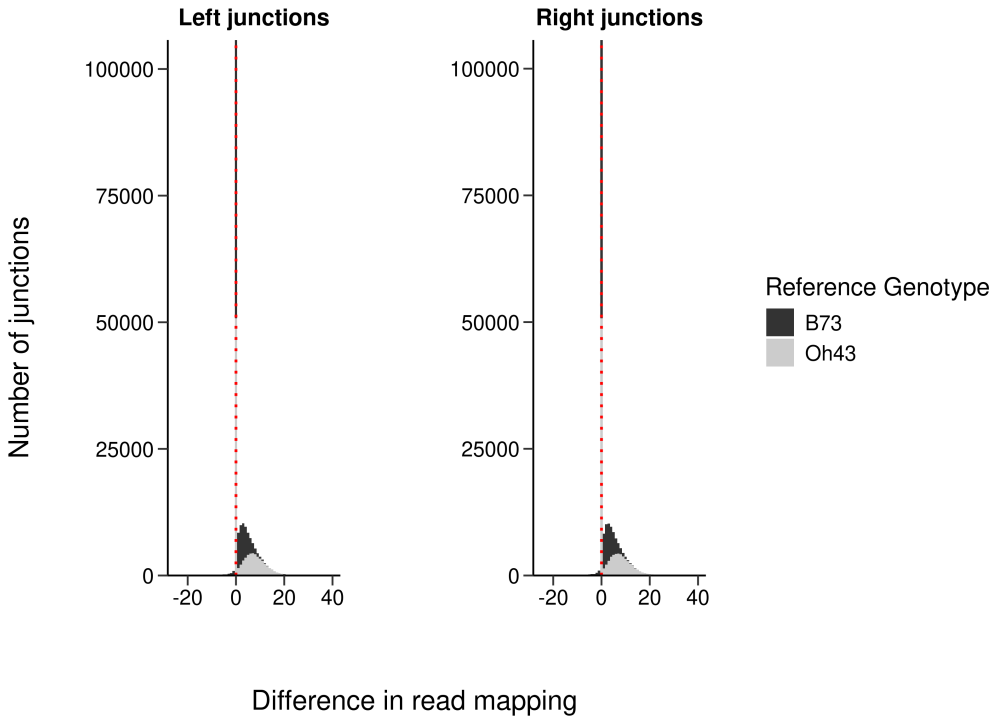

Figure S2. Read mapping differences at the left and right junctions for all SVs – Differences were calculated as the number of reads from the non-parent genotype subtracted from reads mapping from the parent genotype. A positive difference indicates SVs that are supported and retained for future analyses.

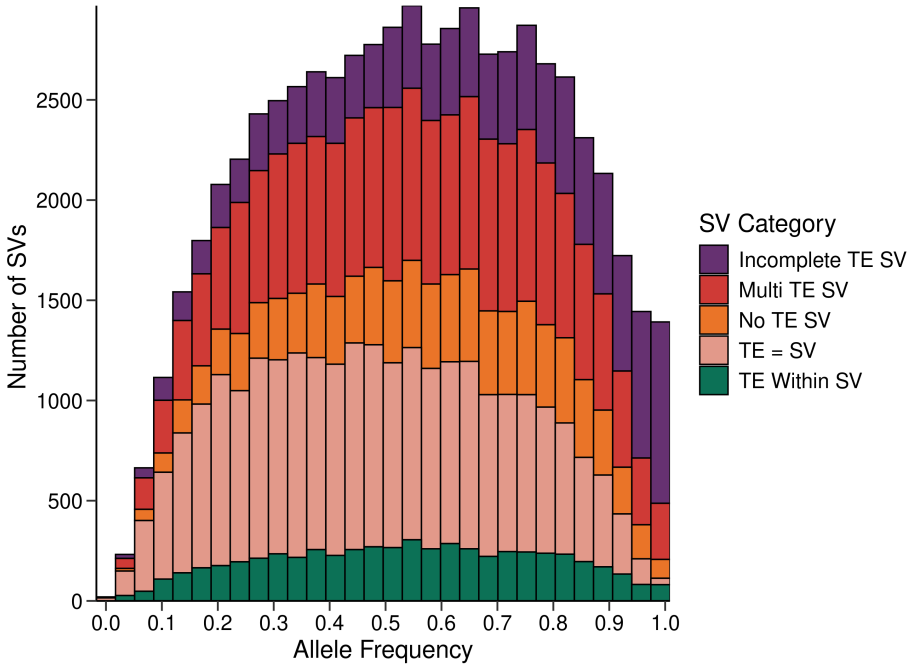

Figure S3. SFS of SVs categorized by TE content – "Incomplete TE SV" and "Multi TE SV" categories SV polymorphisms skew towards moderate to high frequencies whereas all other categories skew towards low to moderate frequencies.

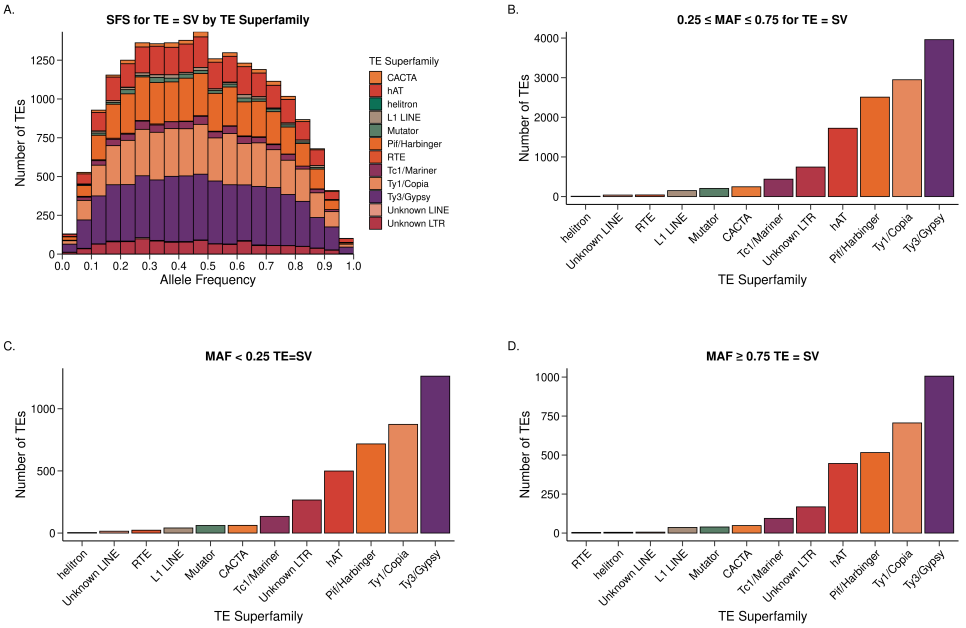

Figure S4. SFS and MAF of TE superfamilies for TE = SV – (A). TE polymophisms skew towards moderate frequency. **(B)**, **(C)**, and **(D)**. Frequencies for all TE superfamilies are consistent across all MAF thresholds.

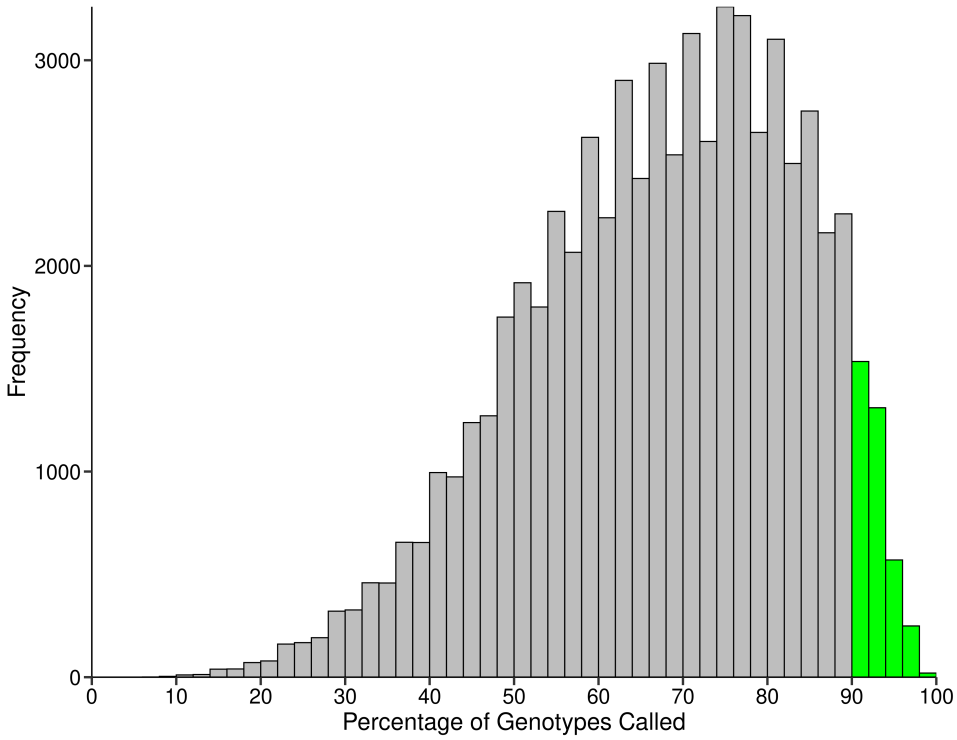

Figure S5. Percentage of genotypes called per SV – Green bars indicate SVs with at least 90% of genotypes called and are retained for GWAS.

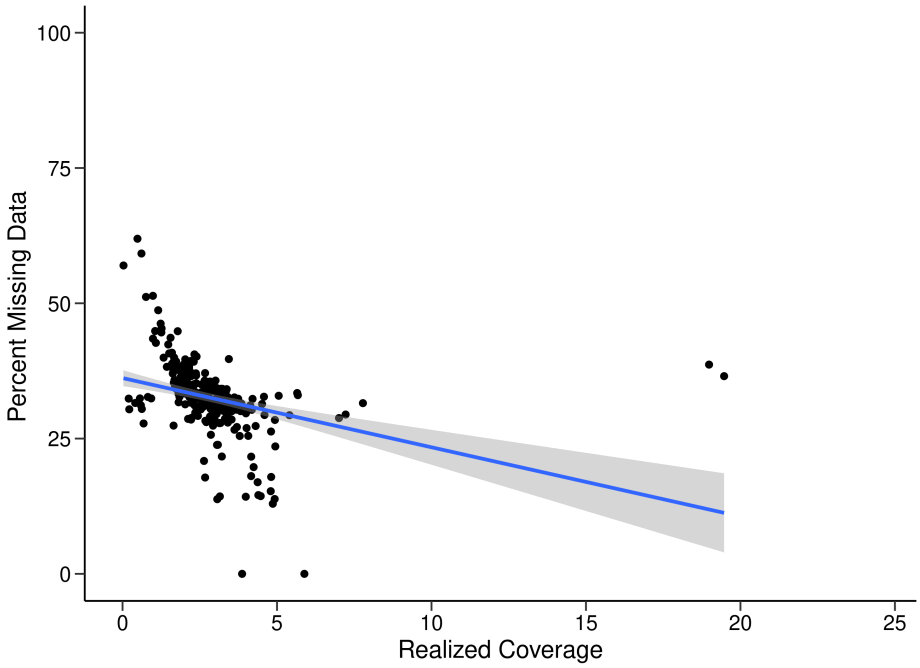

Figure S6. Linear Model of relationship between missing data and read coverage - all genotypes - Adjusted R-squared: 0.1045, F-statistic: 33.20, p-value: 2.22×10^{-8}

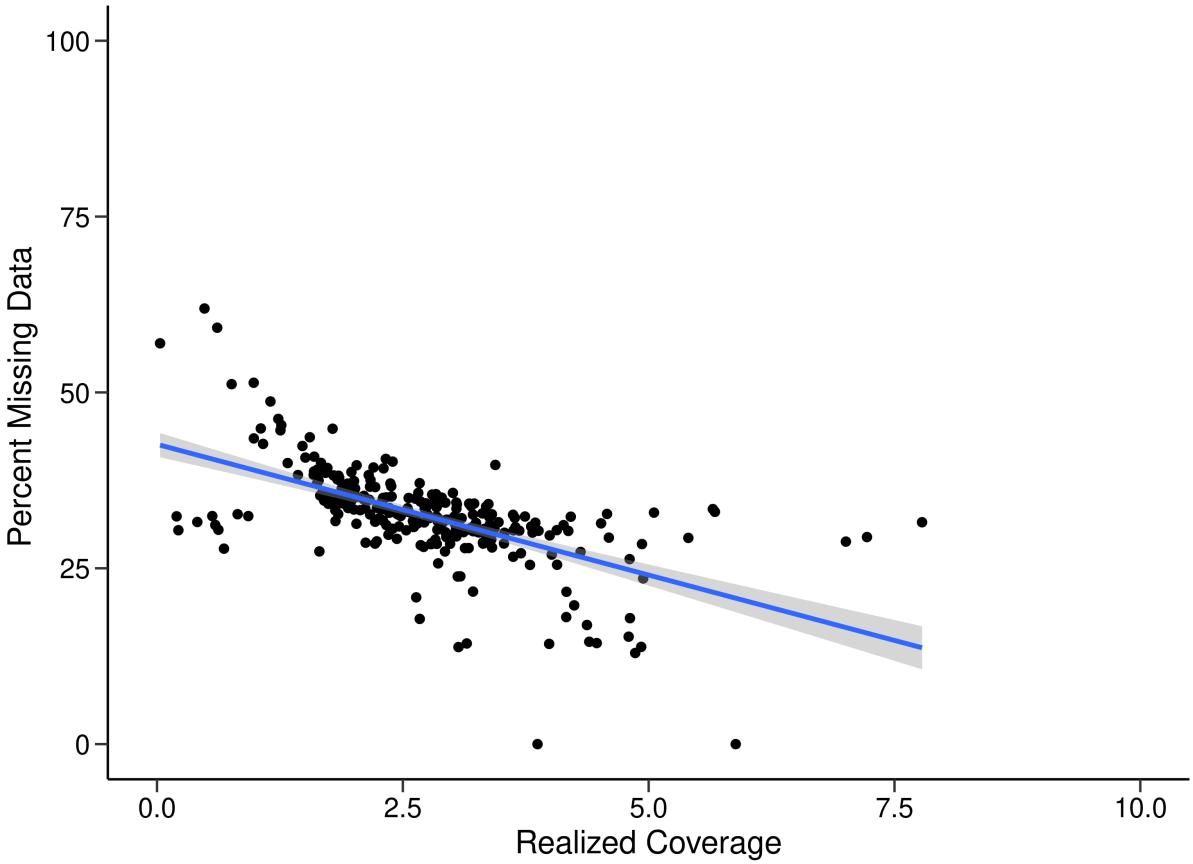

Figure S7. Linear Model of relationship between missing data and read coverage - 2 outliers removed - Adjusted R-squared: 0.3576, F-statistic: 153.50, p-value: 2.2×10^{-16}

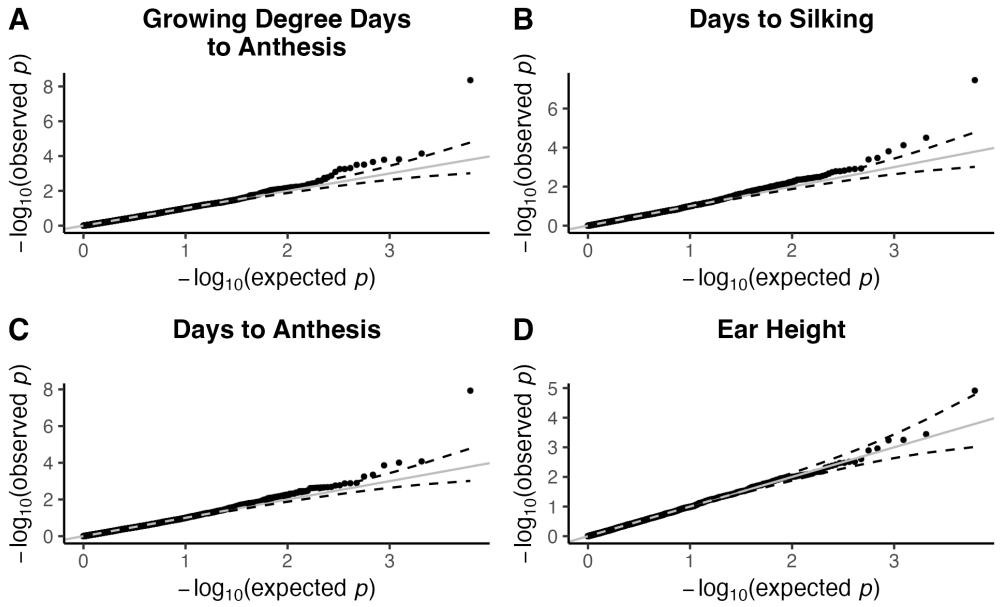

Figure S8. Q-Q plots for traits with SV associations

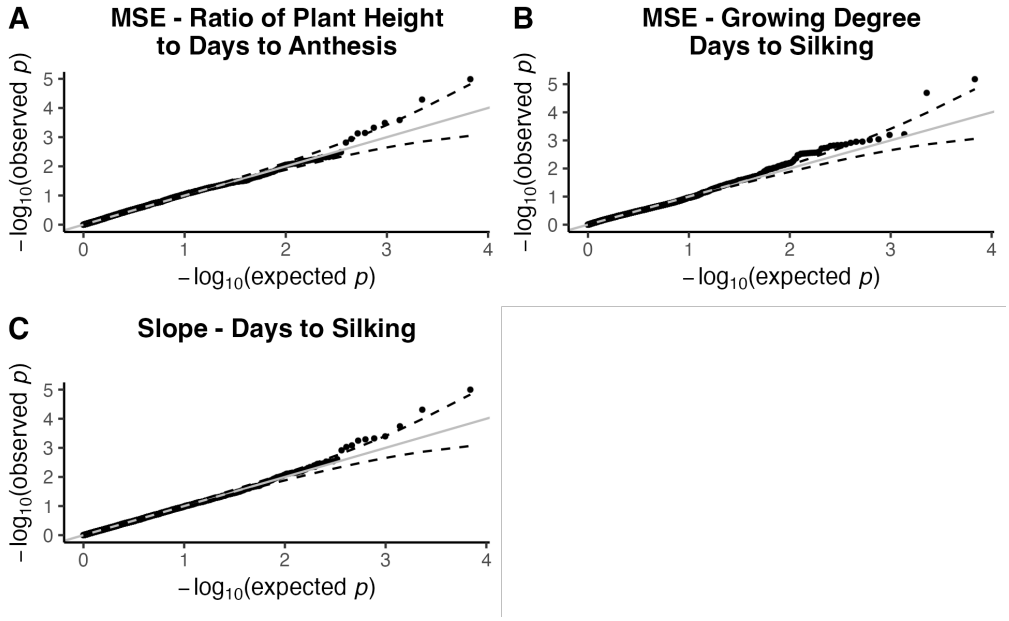

Figure S9. Q-Q plots for Finlay-Wilkinson regression traits with SV associations – (A). the mean-squared error (MSE) of the ratio of plant height to days to anthesis, (B). the MSE of growing degree days to silking, (C). the slope days to silking. Note the deviations between expected and observed p-values in the MSE of growing degree days to silking model (B).

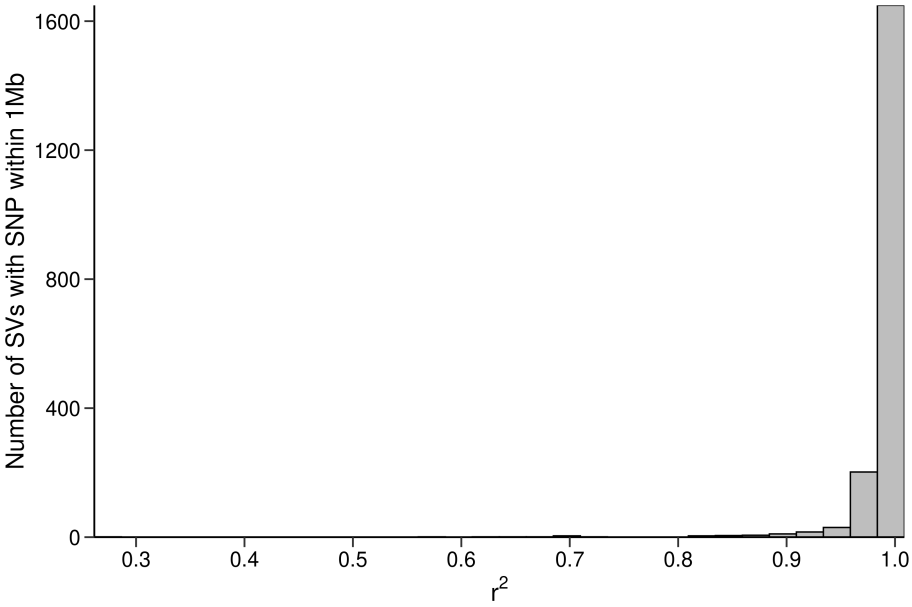

Figure S10. Highest LD between SVs and SNPs within 1Mb – Most SVs used in GWAS are linked with adjacent SNPs

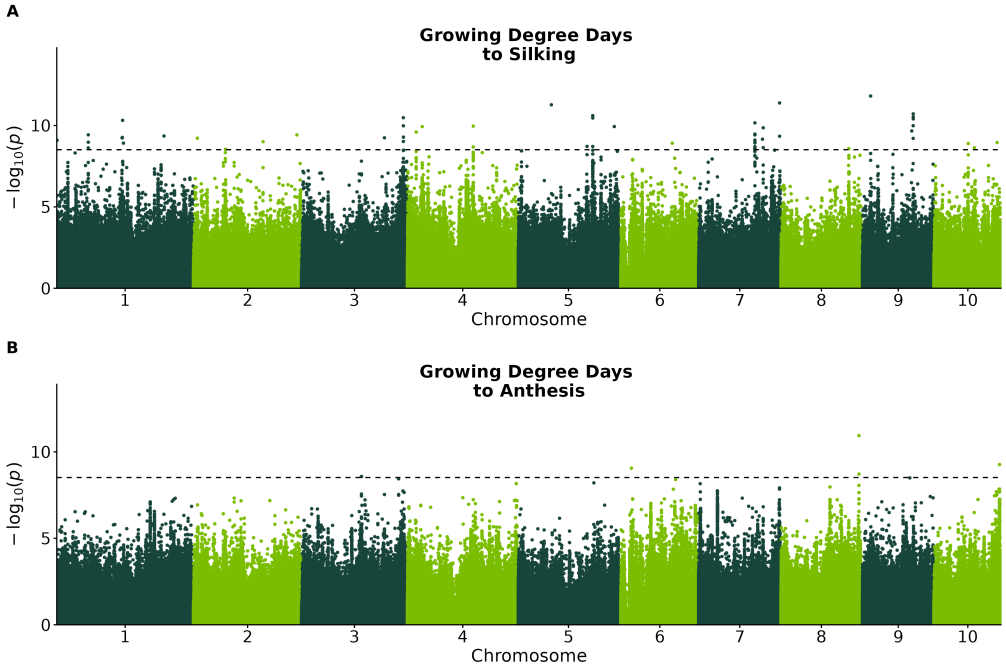

Figure S11. Manhattan Plots of HapMap3 SNPs – (A). There are several SNPs associated with growing degree days to silking, although none are in LD with SVs associated with the same trait. (B). There is a SNP on chromosome 8 associated with growing degree days to anthesis.

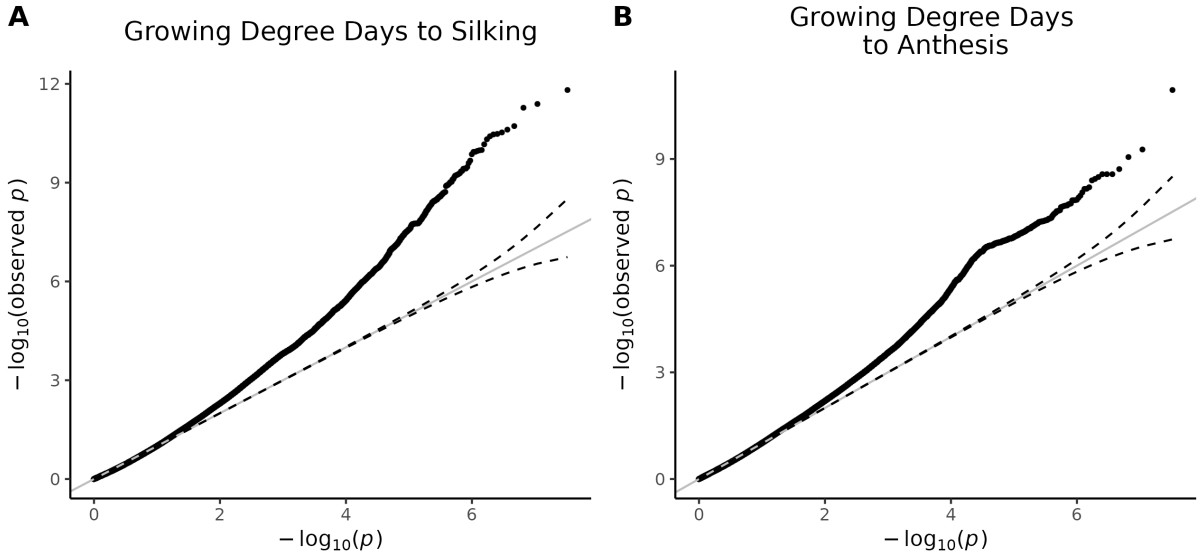

Figure S12. Q-Q plots for traits with HapMap3 SNP associations